



Enhancing surface quality in cutting of gummy metals using nanoscale organic films

Mohammed Naziru Issahaq^d, Anirudh Udupa^d, Tatsuya Sugihara^a, Debapriya Pinaki Mohanty^d, James B. Mann^b, Kevin P. Trumble^d, Srinivasan Chandrasekar^d, Rachid M'Saoubi (1)^{c,*}

^a Department of Mechanical Engineering, Osaka University, Osaka, Japan

^b M4 Sciences Corporation, Lafayette, IN, USA

^c R&D Material and Technology Development, Seco Tools AB, Fagersta, Sweden

^d Center for Materials Processing and Tribology, Purdue University, West Lafayette, IN, USA

ARTICLE INFO

Article history:

Available online xxx

Keywords:

Machining

Surface modification

Organic monolayer embrittlement (OME)

ABSTRACT

A macroscopic ductile-to-brittle transition in chip formation with ductile gummy metals, arising from 3.5 to 100 nm thick organic films on the workpiece surface, is demonstrated. The principal characteristics of the phenomenon, with annealed aluminum, are change in the flow mode from one dominated by large-strain plasticity to one controlled by fracture; and up to 70% reduction in cutting force. This embrittlement has important benefits for machined surface quality – nearly an order of magnitude reduction in roughness, > 50% reduction in residual plastic strain, and smaller hardness change. Implications of the phenomenon for material removal processes and beyond are discussed.

© 2022 CIRP. Published by Elsevier Ltd. All rights reserved.

1. Introduction

A continuous chip of uniform thickness in cutting of metals forms by large-strain deformation typically confined to a narrow shear zone [1]. The underlying material flow, to use a fluid mechanics analogy, is laminar, characterized by homogeneous (uniform) deformation. However, important exceptions to this type of chip formation do exist, wherein the plastic flow is non-uniform [2,3]. Among the latter, of relevance to the present work, are segmentation involving fracture [2,4–6], and sinuous flow with large-amplitude folding and significant redundant deformation [2,7,8].

When cutting very ductile polycrystalline metals such as annealed Al, Cu, Ni alloys and stainless steels, the chip is often very thick ($h_c \sim 10h_0$), with wrinkled “mushroom-like” features on its back surface, see Fig. 1a from linear cutting [2,7–9]. The corresponding chip morphology labeled type 1 is fundamentally different from that of the continuous laminar-flow chip [2]. Type 1 chip formation is often characterized by large cutting forces and poor surface finish despite the workpiece metal being relatively soft [2,7,10]. Recently, utilizing high-speed image photography, the micro/meso scale details of the sinuous flow underlying the type 1 chip have been elucidated [7], reinforcing the important early observations by Nakayama [2]. The flow details have helped explain the large forces and why these metals are “gummy” to cut [7]. Non-uniform flow is also typical of the type 3 saw-tooth or segmented chip (Fig. 1b), which is commonly observed with alloys of low workability (e.g., hard steels, work-hardened brass) [2,4–6]. The segmentation arises from quasi-periodic

fractures that are usually initiated on the workpiece surface ahead of the advancing tool and which then propagate into the chip thickness towards the tool edge [2,3,5]. The occurrence of the fractures limits the plastic deformation (strain) in the type 3 chip – a potential benefit – with the cutting forces also correspondingly being much smaller than otherwise expected [2,10].

At first glance, the type 1 and type 3 chips, standing at opposite ends of the machining spectrum in terms of deformation strain, flow modes and forces, appear to have little in common; and, indeed, this is often the case. However, it has been found recently that with gummy metals such as annealed Al, Cu, Ni and Ta, the typical sinuous-flow (type 1) chip, with large forces/strains, is suppressed and replaced by the segmented-flow (type 3) chip, with much lower forces/strains, if the cutting is done in a suitable environment (medium). Under such conditions, the metal is no longer “gummy” to cut. The chemical media that trigger this flow transition are organic molecules that adsorb (physisorb or chemisorb) onto the surface and form nanometer scale films, that locally “embrittle” the metal (workpiece) surface [11,12]. The embrittling substances, surprisingly, include commonly available chemicals such as permanent marker inks and adhesives. The observations have thus led to a link between the two very disparate flow types, via the embrittling phenomenon termed organic monolayer embrittlement (OME) [12].

In the present study, we explore, in cutting of gummy metals, the principal features of the OME-induced flow-to-fracture transition – a nanometer scale phenomenon, with macroscopic consequences – and how this phenomenon affects machined surface quality. The exploration is guided by the hypothesis that the plastic flow field features, which control chip formation, also determine the machined surface attributes such as finish, residual plastic strain and hardness

* Corresponding author.

E-mail address: rachid.msaoubi@secotools.com (R. M'Saoubi).

(strength). We use annealed Al 1100 workpiece, a prototypical example of a highly ductile gummy metal [13]; cutting at low to moderate speeds (0.3 to 100 m/min); and characterization of material flow and surface attributes, in this exploration. The observations show that the segmented type 3 chip triggered by the OME is beneficial for surface quality – as reflected in smaller roughness, lower residual plastic strain and smaller hardness changes, and reduced density of mesoscale defects (pull-outs, pits). Implications for industrial machining of gummy metals, with applications in energy, chemical, aerospace and orthopedic sectors, are briefly discussed.

2. Experimental

Plane-strain (2-D) cutting, utilizing a linear (shaping) configuration, was used to analyze chip formation, flow modes and workpiece surface quality, with and without chemical media, in low-speed cutting. The cutting parameters were speed $v_c = 300$ mm/min, undeformed chip thickness $h_o = 50$ to 100 μm , rake angle $\gamma = 0^\circ$ to 10° and chip (workpiece) width of 3 to 6 mm. The material flow and deformation underlying chip formation were observed/recorderd from a side of the workpiece with a high-speed camera (Photron FASTCAM Mini WX-100), coupled to a microscope assembly (InfiniFlex with high-definition DS 4x lens of 0.13 NA). The image sequences were analyzed by particle image velocimetry (PIV) to obtain (von Mises) effective strain (ϵ), strain-rate, and rotation fields; flow modes using streaklines; and residual plastic strain in the machined surface/subsurface [7,14] (Note: a streakline is the locus of all particles that have passed earlier through a particular spatial point). Higher speed cutting experiments at $v_c = 100$ m/min, $h_o = 100$ μm , and depth of cut = 0.8 mm, were done using 2-D face turning on a lathe. The flow mode at this speed was inferred from *ex situ* chip morphology observations, based on the established one-to-one correspondence between flow and chip type [2,3]. The cutting forces were measured using a piezoelectric dynamometer (KISTLER, Type 9254). All the experiments were conducted dry without application of any cutting fluid.

The cut surface quality was characterized in terms of surface topography and roughness via optical profilometry (Zygo NewView 9000); residual plastic strain by the PIV; mesoscale defects (material pull-outs, tears) by optical microscopy; and hardness (strength) as a function of depth from the machined surface by Vickers indentation (25 g load). The workpiece material was Al alloy 1100 ($27 \pm 1\text{HV}$, 99% Al) in an initial annealed condition. This alloy is very ductile (uniform elongation $\sim 45\%$) and usually classified as being gummy to machine in the annealed condition [13]. The tool for the low-speed cutting was high-speed steel, and for the higher-speed cutting, a WC–Co cemented carbide. Both tools had cutting-edge radius (~ 5 μm) that was less than $1/10 h_o$.

The chemical media used were a stearic acid monolayer, a permanent marker ink (an adhesive organic film), and isopropyl alcohol (IPA), enabling both thin and ultrathin (nanoscale) films to be formed on the workpiece surface. The stearic acid ($\text{CH}_3(\text{CH}_2)_{16}\text{COOH}$) monolayer of thickness 3.4 nm, as estimated by ellipsometry, was deposited (chemisorbed) onto the initial workpiece surface by a molecular self-assembly method, see Ref. [11] for details. This monolayer is henceforth referred to as Self-Assembled Monolayer (SAM). The ink was applied to the initial workpiece surface with two strokes of the pen and allowed to dry just prior to the cutting. In some of the experiments, this film coating was applied to only part of the cutting length, to observe the flow transition in a single cutting pass. The ink-film thickness was 100 to 200 nm as estimated by optical profilometry. The IPA was applied to the workpiece just after it exited the machining zone; this application was used mainly with the high-speed cutting experiment for ease of studying (inducing) the embrittlement action. The reaction of the IPA with freshly generated Al surfaces results in an ~ 15 nm thick surface layer of aluminum isopropoxide (reaction layer), one of a class of metal alkoxides [15–17]. This oxide is a white solid that melts at 118 °C. The use of the diverse media, all known to induce the OME, was mainly to study film length-scale effects on plasticity/fracture, and the effect of the OME on workpiece surface condition at the different speeds.

3. Results

The experiments have provided interesting insights into the main characteristics of the embrittlement phenomenon mediated by the organic media and its effects on various elements of machined surface quality.

3.1. Principal characteristics of chip formation

Fig. 1 shows select frames from high-speed image sequences of the cutting of the Al at $v_c = 300$ mm/min, with superimposed white streaklines and (von Mises) effective strain field (background). The figure illustrates the embrittlement arising from the stearic acid SAM application. When cutting the bare Al (no film), the chip formed is very thick, with sinewy streaklines and repeated folding (with free-surface ripples) characteristic of the sinuous flow (Fig. 1a, type 1 chip). There is no cracking on the chip free surface, just the occurrence of fold interfaces which could be (and have been) mistakenly interpreted as "cracks". The chip strains are quite large, as high as 6 over a significant part (1/2) of the chip thickness, and highly non-uniform. In contrast, when cutting the ink-coated workpiece, a segmented (type 3) chip occurs, with cracks initiating on the free surface, quasi-periodically, and propagating part way into the chip thickness towards the tool edge (Fig. 1b). The chip now shows much less nominal thickening. It can also be inferred from the strain field, by assigning a representative strain (volume averaged), that this strain value for the segmented chip is only $\sim 35\%$ of that for the sinuous flow chip. The transition from the type 1 to type 3 chip – a local ductile-to-brittle transition – effected by the SAM is a distinguishing characteristic of the embrittlement phenomenon. This characteristic was also seen with the embrittling ink and alkoxide media.

Concomitant with the flow transition from sinuous (highly ductile) to the fracture-dominated segmentation, a large decrease in the cutting force is observed (Fig. 2) – the second distinguishing charac-

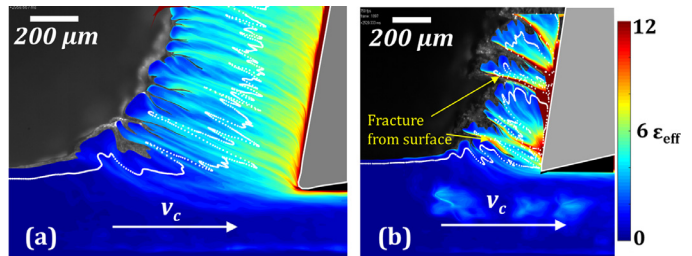


Fig. 1. Image frames of chip formation in linear cutting showing a) sinuous flow (bare), and b) chip segmentation (SAM). Streaklines overlaid against background strain (ϵ) field (color). Al 1100, ($\gamma = 5^\circ$, $h_o = 100$ μm , $v_c = 300$ mm/min).

teristic of the embrittlement. This decrease is as much as 70% due to the organic media. In contrast to the sinuous flow case, Fig. 2 also shows that the force is more stable and uniform with the media, reaching steady state much more quickly. An intriguing feature is that all the media that induce the embrittlement cause essentially the same relative force decrease compared to the bare cutting. If we note that one of the adsorbates is a SAM molecule and another is an alkoxide reaction layer of near-molecular thickness, then it becomes clear that the embrittlement is very likely mediated just by a monomolecular layer that is in immediate contact with the metal surface. This conclusion is reinforced by the very similar results obtained with various other SAMs (molecules) [11,12]. Hence, even with the thicker ink film, it is most likely that the embrittlement is monolayer-induced – by the one-molecule film layer that is intimately adsorbed onto the workpiece surface.

Many of the organic media that triggered the embrittlement were found to have very little commonality in their chemical constituents, ruling out a purely chemical origin for the effect. The observations therefore strongly reinforce the notion of the phenomenon as one of monolayer-induced embrittlement, with the specific medium chemistry being of secondary importance to the phenomenon, and, by

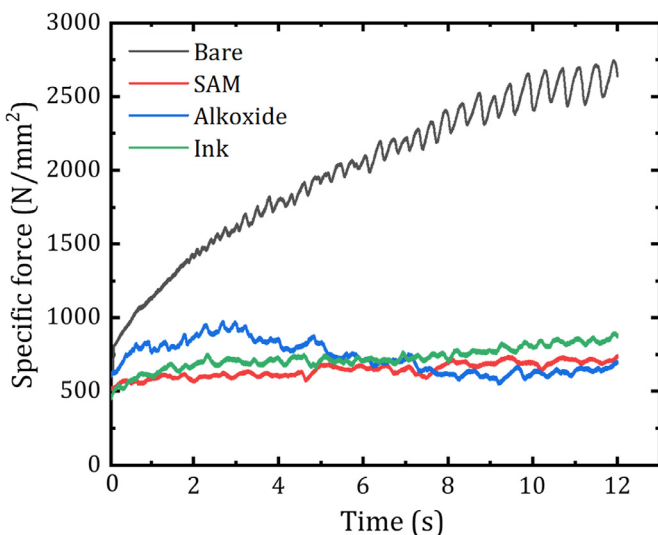


Fig. 2. Specific cutting force with various organic media films/layers ($h_o = 50 \mu\text{m}$, $v_c = 300 \text{ mm/min}$, $\gamma = 10^\circ$). The specific force is the force divided by the undeformed chip cross-section area.

extension, to its consequences. Henceforth, we will refer to this phenomenon as the OME to emphasize the key role of the monolayer.

3.2. Surface finish and topography

Fig. 3 shows optical profilometry images of the workpiece surfaces. The top row is for the low-speed cutting without and with the OME, while the bottom row is an equivalent set for the higher-speed case. In the top row, the initial part ($\sim 50\%$) of the workpiece length was bare, while the remaining part was coated with the ink (OME) prior to the cutting. The contrast between the roughness in the two regions (top row, **Fig. 3**) is quite dramatic. The cut surface corresponding to the bare region is characterized by deep pits and pull-outs, with peak-to-valley $Rz \sim 93 \mu\text{m}$. The latter is based on 20-line scans across the topography. The corresponding Ra value is not reported given the very rough nature of the cut surface. The linear density of defects (tears, pull-outs, pits) on the cut surface, as determined from the profilometry and optical microscopy, was $\sim 0.35/\text{mm}$. The cut surface in the coated region is significantly smoother, with $Rz \sim 1.34 \mu\text{m}$ and $Ra \sim 0.2 \mu\text{m}$. Furthermore, there is very little evidence of any surface damage (e.g., pull-outs or tears) on this surface; in fact, the measured linear defect density was essentially zero. The low-speed cutting results specifically highlight an extraordinary, nearly 1.5 order of magnitude, improvement in the surface roughness arising from the OME.

The improvement in surface roughness enabled by the OME was also found to occur in the higher speed cutting with $v_c = 100 \text{ m/min}$ (bottom row, **Fig. 3**). In this experiment, the IPA was applied to the

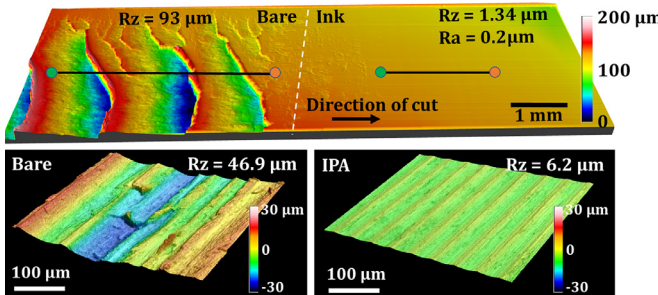


Fig. 3. Cut surface topography without and with the OME. Top row: low cutting speed - 300 mm/min . Bottom row: higher cutting speed - 100 m/min ($\gamma = 10^\circ$, $h_o = 100 \mu\text{m}$).

workpiece in and around the process zone, so that the freshly cut Al surface emerging from this zone could immediately react with the

alcohol. The workpiece surface entering the process zone for the next cutting pass is thus covered with an alkoxide layer, enabling the OME. The Ra value on the cut surface from the alkoxide-coated region is $\sim 1.18 \mu\text{m}$ ($Rz \sim 6.2 \mu\text{m}$), representing a greater than 5-fold reduction in roughness compared to the bare case, $Ra \sim 8.3 \mu\text{m}$ ($Rz \sim 46.9 \mu\text{m}$). Furthermore, as in the low-speed cutting, the density of surface defects on the cut surface is also significantly reduced by the OME. In fact, the bottom row of the figure shows essentially no macro or meso scale defects on the cut surface in the alkoxide-coated region. The other distinguishing characteristics of the OME – drop in the cutting force and change in the chip morphology – were also observed in these higher speed experiments. Although not shown here, a segmented chip, typical of the OME, resulted in the alkoxide (IPA) case, whereas the chip showed the sinuous flow characteristic in the bare case. Concurrently, an $\sim 33\%$ reduction in the cutting force was observed with the IPA. This reduction, while somewhat smaller than the 70% reduction observed in the low-speed cutting due to the OME, is still quite substantial.

The higher speed cutting results show that the OME can, potentially, be quite effectively used even at industrial cutting speeds provided a monolayer of the “right” organic medium can be adsorbed sufficiently rapidly on the workpiece surface (or equivalently chemical reaction layer formed) between successive cuts. This, however, will be very much determined by factors such as adsorption kinetics of the medium and mode of medium application, besides of course, the core ability of the medium to trigger the OME with the specific workpiece metal. Further experiments are planned to determine the speed limit, if any, at which the OME “disappears”.

3.3. Surface strain and hardness

We now turn our attention to another very important element of machined surface quality – surface integrity – which is largely determined by the plastic deformation state of the surface [18]. Since the OME changes the plastic flow mode and deformation state in the chip quite dramatically, it is reasonable to expect that the residual deformation state of the machined surface will also be significantly altered. We characterized the surface integrity using two measures – the residual plastic strain on the cut surface and the near-surface hardness which is directly influenced by this strain. To quantify this plastic strain, we employed the same approach as that used to obtain the strain field in the chip. Using the PIV high-speed image analysis, we tracked path lines followed by material elements that enter the workpiece near-surface at various depths in the wake of the tool. The residual strain on the cut surface is then obtained by accumulating the incremental strain along these path lines [14].

Fig. 4a shows the variation of residual plastic strain with depth from the surface. The OME effect is quite significant. The maximum strain in both cutting cases, i.e., with and without the OME, occurs at the surface. The strain value is ~ 3.25 when cutting the bare Al and ~ 1.4 when cutting with the OME, representing a nearly 60% reduction in the strain due to the OME. In both cases, the strain is seen to decrease smoothly and monotonically with depth from the surface. If we define the deformed region as that part of the sub-surface with strain > 1 , then the thickness of the deformed region in the OME case is $\sim 25 \mu\text{m}$. In comparison, the corresponding thickness for the bare Al case is much greater than $60 \mu\text{m}$ (Note: the $60 \mu\text{m}$ depth is the maximum depth over which the strain distribution was measured). Thus, the OME causes a significant reduction not only in the maximum surface strain, but also a concomitant reduction in the depth of the intensely deformed surface layer. It may be of interest to note here that we have observed even larger decreases in these two attributes – maximum surface strain and deformed layer thickness – of the strain field intensity in machined Cu, also due to the OME.

($h_o = 50 \mu\text{m}$, $v_c = 300 \text{ mm/min}$, $\gamma = 10^\circ$)

Measurements of the cut surface hardness and its variation with depth into the subsurface showed a pattern consistent with the strain field intensity (**Fig. 4b**). But the strengthening by the residual plastic deformation is only about 35%, with respect to the (baseline) bulk

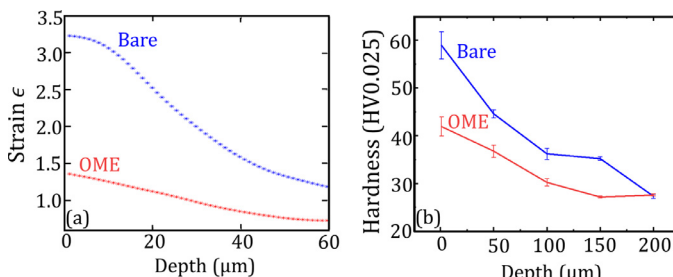


Fig. 4. Variation of a) strain and b) hardness with depth into the workpiece subsurface, with and without OME-enabling film.

annealed Al, in the OME case. Whereas in the bare Al case, the corresponding strength increase is > 100%, in keeping with the larger surface strain here. These strength changes closely mimic the strain patterns on the two cut surfaces. The strain-field and the closely correlated hardness observations suggest that the OME-enabled cutting could be a viable approach for producing “minimally strained” surfaces. This could be of value not only for enhancing performance of structural and mechanical components, but also for specimen preparation procedures. Another consequence of the OME residual strain field is that it could facilitate more stable chip formation by eliminating the chip thickness oscillations sometimes observed with soft Cu, Ta and Nb [7]. Indeed, we have noted such a stability improvement in OME-enabled turning experiments involving these metals.

4. Summary, observations and implications

The study of cutting of Al 1100 in the presence of organic media such as permanent marker ink, isopropyl alcohol and stearic acid has shown an interesting local ductile-to-brittle transition in material behavior mediated by nanoscale (3.5 nm to 100 nm) surface films. This ductile to brittle transition, labelled organic monolayer embrittlement (OME), is truly a nanoscale phenomenon - a visible macroscopic change in the mechanical behavior of the metal triggered by nanometer-scale films. Its principal characteristics are a) effecting a change in chip type from one controlled by sinuous, large-strain plastic flow (ductile) to one of fracture-controlled segmentation with much lower primary deformation zone strain; and b) corresponding large-reductions of up to 70%, in the cutting force. The OME characteristics are largely independent of the medium chemistry, as long as the phenomenon is enabled by the adsorption or chemical reaction. The OME has important benefits for machined surface quality, including 5 to 10 fold reduction in the principal roughness parameters; significantly reduced density of surface defects such as pull-outs and pits; > 50% reduction in plastic strain and deformed layer thickness on the cut surface; and smaller changes in hardness of the machined surface. A limited set of experiments has shown that the benefits of the OME for surface quality can also be realized at industrial cutting speeds. The results thus indicate that the OME can be quite beneficial for cutting of gummy metals, impacting industry sectors as diverse as aerospace, energy and orthopaedics.

The OME likely belongs to one of the many chemical effects that have been suggested to occur in material removal processes [19–23]. However, the specificity of the effect with the nanoscale films shows that there is now a metrology tool (self-assembled monolayers (SAMs)) available to systematically probe the effect. That it can occur with common benign (household) media that are non-corrosive, and which do not embrittle the residual cut surface (in contrast to say liquid gallium), suggests applications opportunities, not only for cutting, but also for other material removal processes such as grinding, polishing and comminution. While the mechanism underlying the OME is not yet fully known, there is emerging evidence to suggest that it

arises from a tensile surface stress locally generated by the film [11,12]. The surface stress is a thermodynamic parameter, the analogue of surface tension for solids. Another outstanding question pertains to the specific molecule chemistry needed to enable the effect. The OME has implications beyond cutting, perhaps, playing an important role in mediating well-known environmentally assisted cracking (EAC) phenomena such as stress-corrosion cracking, hydrogen embrittlement and liquid metal embrittlement [19,23]. And for the authors, there are other important lessons that have been learned: benign household media like inks and glues can be potent in a good way; and one should be careful when routinely and casually marking metal surfaces with ink – you may be unwittingly embrittling it!

Declaration of Competing Interest

The authors declare that they have no known competing financial interests or personal relationships that could have appeared to influence the work reported in this paper.

Acknowledgement

The research was supported in part by NSF grants DMR 2104745 and CMMI 2100568 to Purdue University.

References

- [1] Shaw MC (2005) *Metal Cutting Principles*, Oxford University PressNew York.
- [2] Nakayama K (1974) The Formation of Saw-Toothed Chip in Metal Cutting. *Proceedings of the International Conference on Production Engineering*, Tokyo 1:572–577.
- [3] Viswanathan K, Udupa A, Yeung H, Sagapuram D, Mann JB, Saei M, Chandrasekar S (2017) On the Stability of Plastic Flow in Cutting of Metals. *Annals of the CIRP* 66 (1):69–72.
- [4] Nakayama K, Arai M, Kanda T (1988) Machining Characteristics of Hard Materials. *Annals of the CIRP* 37(1):89–92.
- [5] Shaw MC, Vyas A (1993) Chip Formation in the Machining of Hardened Steel. *Annals of the CIRP* 42(1):29–33.
- [6] Davies MA, Burns TJ, Evans CJ (1997) On the Dynamics of Chip Formation in Machining Hard Metals. *Annals of the CIRP* 46(1):25–30.
- [7] Yeung H, Viswanathan K, Compton WD, Chandrasekar S (2015) Sinuous Flow in Metals. *Proceedings of the National Academy of Sciences* 112(32):9828–9832.
- [8] Okushima K, Hitomi K (1957) On the Cutting Mechanism for Soft Metals. *Memoirs of the Faculty of Engineering* 19:135–166. Kyoto University.
- [9] Williams JE, Smart EF, Milner DR (1970) Metallurgy of Machining. Part 1: Basic Considerations and the Cutting of Pure Metals. *Metallurgia* 81:3–10.
- [10] Nakayama K, Takagi J, Nakano T (1974) Peculiarity in Grinding of Hardened Steel. *Annals of the CIRP* 23(1):89–90.
- [11] Sugihara T, Udupa A, Viswanathan K, Davis JM, Chandrasekar S (2020) Organic Monolayers Disrupt Plastic Flow in Metals. *Science Advances* 6(51):eabc8900.
- [12] Udupa A, Sugihara T, Viswanathan K, Latanision RM, Chandrasekar S (2021) Surface-Stress Induced Embrittlement of Metals. *Nano Letters* 21(22):9502–9508.
- [13] Handbook ASM (1989) *Machining of Aluminum and Aluminum Alloys*, 16, ASM International, 761–804.
- [14] Guo Y, M'Saoubi R, Chandrasekar S (2011) Control of Deformation on Machined Surfaces. *Annals of the CIRP* 60(1):137–140.
- [15] Bradley DC (1959) Metal Alkoxides. *Progress in Inorganic Chemistry* 2:303–361.
- [16] Montgomery RS (1965) The Effect of Alcohols and Ethers on the Wear Behaviour of Aluminium. *Wear* 8:466–473.
- [17] Strawhecker K, Asay D, McKinney J, Kim S (2005) Reduction of Adhesion and Friction of Silicon Oxide Surface in the Presence of N-Propanol Vapor in The Gas Phase. *Tribology Letters* 19(1):17–21.
- [18] Jawahir IS, Brinksmeier E, M'Saoubi R, Aspinwall DK, Outeiro JC, Meyer D, Umbrello D, Jayal AD (2011) Surface Integrity in Material Removal Processes: recent Advances. *Annals of the CIRP* 60(2):603–626.
- [19] Rehbinder PA, Shchukin ED (1972) Surface Phenomena in Solids During Deformation and Fracture Processes. *Prog Surf Sci* 3(2):97–188.
- [20] Usui E, Gujral A, Shaw MC (1961) An Experimental Study of the Action of CCl_4 in Cutting and Other Processes Involving Plastic Flow. *International Journal of Machine Tool Design and Research* 1(3):187–197.
- [21] Brinksmeier E, Lucca DA, Walter A (2004) Chemical Aspects of Machining Processes. *Annals of the CIRP* 53(2):685–699.
- [22] Coes L (1955) Chemistry of Abrasive Action. *Industrial & Engineering Chemistry* 47 (12):2493–2494.
- [23] Latanision RM, Fourie JT, (Eds.) *Surface Effects in Crystal Plasticity*, Noordhoff International Publishing.